

## Gap anisotropy of $\text{Bi}_2\text{Sr}_2\text{CaCu}_2\text{O}_8$ measured by low-temperature scanning tunneling microscopy

Qun Chen and K.-W. Ng

*Department of Physics and Astronomy, University of Kentucky, Lexington, Kentucky 40506-0055*

(Received 10 October 1991)

Energy gaps of single-crystal  $\text{Bi}_2\text{Sr}_2\text{CaCu}_2\text{O}_8$  in the  $c$ -axis and the  $ab$ -plane directions are measured directly by the scanning-tunneling-microscopy method. Due to the short coherence length along the  $c$  axis, conductance curves in this direction are seriously smeared and do not fit the conventional BCS density of states. In the  $ab$  direction, the shapes of the conductance curves are different from that of  $c$ -axis tunneling and show sharper gap features. The energy gap in the  $ab$  direction is measured to be 35 meV, which is 10 meV larger than the value in the  $c$ -axis direction.

Gap anisotropy can provide direct information on the direction dependence of the pairing potential. There have been limited reports on the observation of gap anisotropy by tunneling methods. Most of these measurements showed only small energy-gap differences in different tunneling directions.<sup>1</sup> It is believed that the anisotropic effect was smeared out by scattering processes. In most cases, the general condition of  $l \gg \xi$ , where  $l$  is the mean free path and  $\xi$  is the coherence length, was not satisfied. However, in the case of high- $T_c$  superconductors, the coherence lengths are much shorter than for other conventional superconductors. Despite the fact that the short coherence length causes tunneling measurements to be very surface sensitive (especially in the  $c$ -axis direction), it is more likely for the gap anisotropy to be observed in the high- $T_c$  materials.<sup>2</sup>

Direction dependence of energy gap is particularly interesting for cuprate high- $T_c$  superconductors because it is widely accepted that these materials show extraordinary anisotropic effects due to the Cu-O layer structure. Indirect measurements of coherence lengths in perpendicular and in-plane directions demonstrate that  $\text{Bi}_2\text{Sr}_2\text{CaCu}_2\text{O}_8$  (BSCCO or 2:2:1:2) is one of the highest anisotropic members in this class of superconductors.<sup>3</sup> One possible reason is due to the larger separation between Cu-O planes in the BSCCO system. For the same reason, the BSCCO single crystal can be easily cleaved to obtain a clean surface before taking measurements. BSCCO is also more stable against oxygen deficiency than other high- $T_c$  superconductors. In this paper we will report tunneling results on BSCCO system in both  $c$ -axis and  $ab$ -plane directions.

There have been numerous reports of studies on BSCCO by different tunneling methods, including conventional sandwich-type junctions,<sup>4-7</sup> breakable junctions,<sup>8</sup> point contacts,<sup>9,10</sup> and scanning tunneling microscopy and spectroscopy.<sup>11</sup> The energy gap values varied from 20 to 50 meV because of different phases in the samples. The value we report here is in agreement with those from several articles published recently.<sup>4,6,12,13</sup> Shapes and detail features of the conductance curves varied in these reports. Many measurements<sup>6,9</sup> have a parabolic background in the conductance curves, probably due to the particularly low work function of this material<sup>14</sup> and relatively large tunneling bias. Multiple gaps<sup>4,15</sup> and oth-

er fine features<sup>16,17</sup> were often observed. However, none of these features can be observed repeatedly.

Although some authors used gap anisotropy to explain the gap differences in their results,<sup>9</sup> only a few reported<sup>8,12,15,18</sup> direct measurements of the gap anisotropy by tunneling in different directions. As pointed out by Mandrus *et al.*,<sup>8</sup> direction of tunneling in these measurements was not well defined because the tip could penetrate the surface. To avoid similar problems, we approached the tip carefully towards the sample surface ( $ab$ -plane) and all measurements were performed at very high junction resistances, in the range of 10 M $\Omega$ . For in-plane tunneling, the tip was replaced by a BSCCO sample and tunneling occurred between edges of the two high- $T_c$  samples. Since the BSCCO quasiparticle density of states is not known, experimental results may be more reliable for tunneling between BSCCO and a more conventional superconductor. NbSe<sub>2</sub> was chosen for this purpose because of its BCS-like density of states and the quasi-two-dimensional layer structure.

A home-built low-temperature scanning tunneling microscope (STM) was used in all measurements described in this paper. The STM has a single piezoelectric tube scanner design and a cylindrical shape to minimize horizontal drifting. It is installed inside a vacuum container with springs for vibrational isolation. At the top is a small exchange chamber through which samples and tips can be transferred and replaced while the STM and the vacuum container are in the liquid-helium bath. Coarse  $z$ -direction motion is obtained by turning the sample screw with a step motor and gear system from the outside. To avoid a crash between the tip and sample, the tip has to be withdrawn before the temperature is raised. Despite differences in the shapes of the tunneling conductance curves, positions of the peaks can be consistently reproduced.

Samples were prepared by Tao *et al.* at Polytechnic University using method reported by Mitzi *et al.*<sup>19</sup> Sizes of samples were about  $5 \times 5 \text{ mm}^2$ , 0.1 mm in thickness.  $T_c$ 's of samples were determined after tunneling measurements by resistivity method to be 85 K. The STM was operated in its regular mode when the energy gap was probed in the  $c$  direction. Tunneling occurred between the normal Pt-Ir tip ( $N$ ) and BSCCO ( $H$ ) sample (perpendicular to the tip) in the  $c$  direction [Fig. 1(a)]. Each

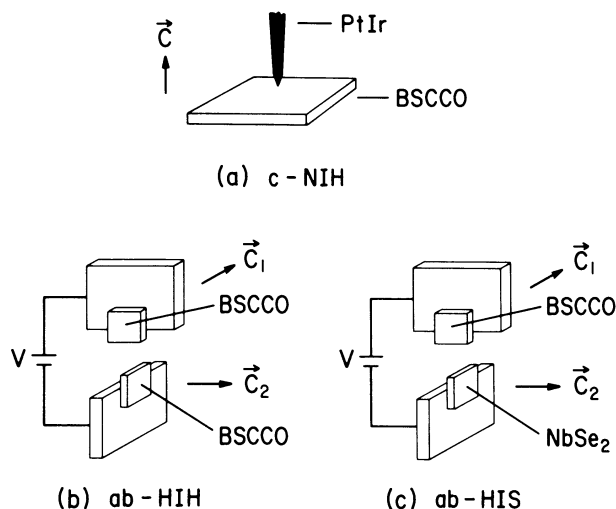


FIG. 1. Tunneling on single-crystal BSCCO in different directions. (a) The STM in its regular configuration with the Pt-Ir tip ( $M$ ) along the  $c$  axis of the BSCCO sample ( $H$ ). (b) The tip is replaced by another piece of BSCCO sample and assembled in a cross configuration. (c) One of the BSCCO samples is replaced by another layer structure superconductor  $\text{NbSe}_2$ .

sample was cleaved to obtain a clean, flat surface before measurement and immediately transferred to the low-temperature STM at 4.2 K.

For  $ab$ -plane to  $ab$ -plane tunneling ( $ab$ -HIH), a BSCCO sample was cut into two pieces. The STM was configured in such a way that the Pt-Ir tip was replaced by one piece of the BSCCO samples, with  $ab$  plane parallel to the original tip direction. The second piece of sample was mounted so that the freshly cut edges of the two samples face each other, forming a cross structure [Fig. 1(b)]. Samples were observed under optical and electron microscopes after each experiment to ensure the edges were well formed and not damaged during the experiment. The use of STM allowed us to control the junction resistance precisely, and change location of the junction microscopically. The same configuration and procedure were applied to the case of BSCCO- $\text{NbSe}_2$  ( $ab$ -HIS) in-plane tunneling [Fig. 1(c)].

Figure 2(b) shows a typical  $c$ -direction tunneling ( $c$ -NIH) conductance curve for BSCCO. Most of our  $c$ -NIH curves have a V-shaped gap opening and feature nonzero conductance at zero bias. Since the coherence length is very short in the  $c$  direction, all  $c$ -NIH tunneling curves are smeared out. At high junction resistance, when the tip is distant from the sample, gap features disappear and only a V-shaped background remains [Fig. 2(a)]. Similar normal-state features have been observed by many other authors with other high- $T_c$  materials.<sup>20,21</sup> None of the  $c$ -NIH curves is close to BCS-like, even within the gap region. Thus it is not possible to fit any of these curves with a BCS density of state and a Lorentzian-type broadening. There is no legitimate way to extract the energy gap without knowing the correct density of states, and the mechanism that causes the smearing. In this paper, the energy gap is determined by the posi-

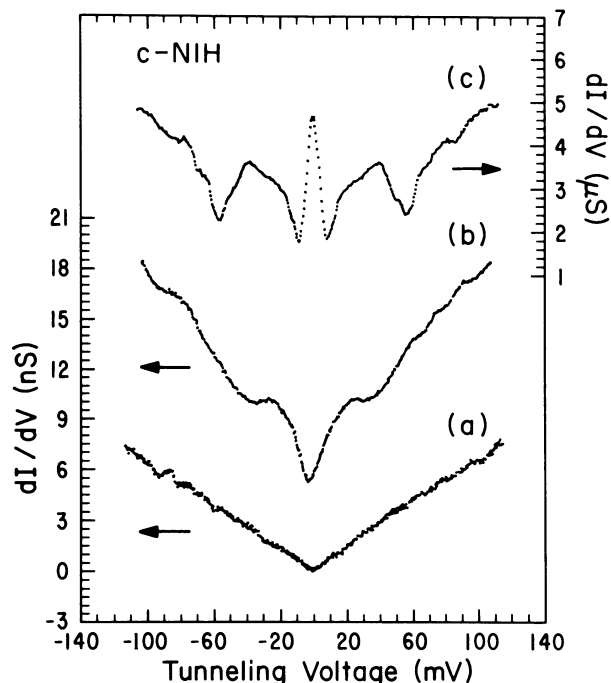


FIG. 2. Tunneling curves for  $c$ -NIH tunneling. (a) A V-shaped conductance curve is always observed at very high junction resistance. (b) The energy-gap feature will appear as the junction resistance is reduced by controlling the piezoelectric tube. (c) As one continues to reduce junction resistance, many fine features will start to appear on the conductance curve. Except for the zero-bias anomaly, none of these features can be repeated consistently. The sample surface is basically damaged when these features start to appear.

tions of the peaks in the conductance curve. From the tunneling curve shown in Fig. 2(b), the gap value in  $c$  direction is measured at 25 meV.

All conductance curves in this tunneling direction have a background increasing with bias voltage, which can be either linear or paraboliclike. This is an interplay between density-of-states characteristics, scattering, and low work function. To examine the differences between high and low junction resistance, the tip was driven closer to the surface down to a junction resistance of 1 k $\Omega$  in some experiments. At such a low resistance, the surface was actually cracked by the tip. Conductance curve from one of these surface broken junction is shown in Fig. 2(c). The Josephson-like zero-bias anomaly can generally be repeated over different junctions. This can be due to the Josephson coupling between particles of BSCCO sample, or by proximity induced Josephson tunneling.<sup>22</sup> Signature of the superconducting gap can still be traced in Fig. 2(c). However, it is heavily covered by other more pronounced features. Until now there is no strong evidence that any of these features can be reproduced or related to the material properties.

There are two factors that contribute to gap anisotropy in superconductors. One is the direction dependence of the pairing potentials  $V_{\mathbf{k}\mathbf{k}'}$ , which is believed to be highly anisotropic in high- $T_c$  materials. The other factor to be considered is the geometry of the Fermi surface. These

two factors can counterbalance each other and cause the anisotropy in energy gap to be less pronounced in comparison with that of coherence length, or results from other transport measurements. The difficulty of tunneling is in obtaining consistency in the measurement of the energy gap, with an error less than the difference of gap values in the two perpendicular directions. As we pointed out in an earlier paper,<sup>13</sup> in the case of BSCCO, energy gap can be repeatedly measured within several meV if one approaches the tip towards the surface carefully and perform the measurements at high junction resistance. The small discrepancy is due to different phases of different  $T_c$  in the sample, and smearing effects.

*ab*-HIH junctions produce sharper conductance curves (Fig. 3) than those of *c*-NIH junctions. Junction resistance is smaller than the *c*-NIH resistance because of the larger tunneling area. No energy gap can be observed for junctions with resistance larger than 5 M $\Omega$ . Since this maximum resistance is in general smaller than that of point junction *c*-NIH, we have to conclude that the barrier width (but not noises or resistance) plays an important role in the smearing out of the energy gap. The peak position is given by the sum of the gap, which is equal to  $2\Delta_{ab}$  in the present case. The energy gap in the *ab*-plane direction is measured to be 33 meV. This is substantially larger than that in the *c* direction. We should point out that although the curves in Fig. 3 have a flat normal-state

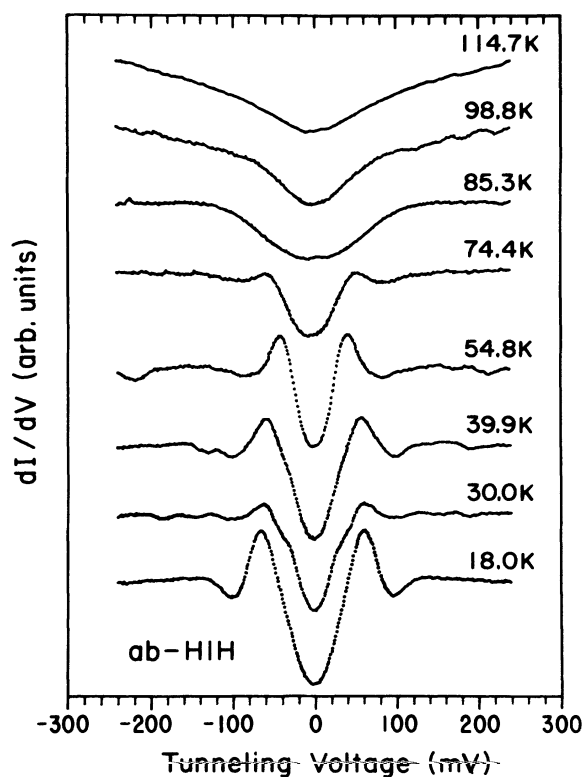


FIG. 3. Typical tunneling curves of *ab*-HIH tunneling. This is a collection of conductance curves at different temperatures in the same run of experiment. The energy gap is given by the difference of peak positions divided by 4, which is equal to 33 meV.

background, parabolic background has also been seen in other junctions of the same structure. Figure 3 shows a sequence of conductance curves at different temperatures. Samples have been separated mechanically and reapproached as the temperature is changed, thus one should view these curves as different junctions. The small feature within the gap in the 30.0-K curve may correspond to the inner gap structure in Ref. 4, or due to some components of NIH tunneling. However, this inner gap feature cannot be reproduced in other measurements. The major gap feature broadens with increasing temperature and disappears at  $T_c$ . Note that the peak for 74.4 K is at an outer region than that of 54.8 K, because the gap enhancement due to thermal smearing effect is more significant than the actual decrease of energy gap in this temperature range.

Since the mechanism and density of states of the high- $T_c$  materials are not well established, we also performed BSCCO-NbSe<sub>2</sub> (*ab*-HIS) tunneling in similar cross configuration to avoid the potential complication due to tunneling between two high- $T_c$  materials. As can be seen from Fig. 4, the energy gap measured basically supports our previous *ab*-HIH results, with a value around 35 meV. It is slightly larger than the *ab*-HIH value because of the NbSe<sub>2</sub> gap. The peak for  $\Delta_{\text{BSCCO}} - \Delta_{\text{NbSe}_2}$  is too small and too close to the major peak of  $\Delta_{\text{BSCCO}} + \Delta_{\text{NbSe}_2}$  for it to be resolved. Unlike many results from sandwich-type conventional junctions, we observe no peak near zero bias due to the conventional superconductor.

Comparing the gap values in *c* and *ab* directions (Fig. 4), we can see a difference of 10 meV. This gives a reasonable lower bound of estimations on gap anisotropy. Deviations from BCS density of states (especially in the *c* direction) forbid us from using any existing mean to extract the energy gap value. Judging from the fact that the

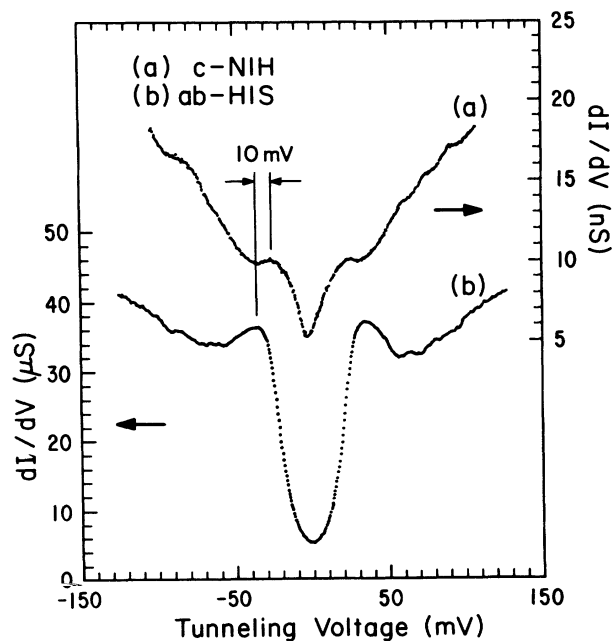


FIG. 4. The lower curve is from *ab*-HIS tunneling. The energy-gap value is consistent with that from *ab*-HIH tunneling. The *c*-NIH curve is put at the top in the same energy scale to show the difference in the peak positions.

*c*-axis conductance curve is more dispersed than that of *ab* plane, the real difference between the directions should be larger than the above value.

We gratefully thank Dr. H. J. Tao, Dr. Farun Lu, and Dr. E. L. Wolf of Polytechnic University in providing the

BSCCO samples for this experiment. SEM work was performed in the Center for Applied Energy Research (University of Kentucky). We also want to express our appreciation to G. Mathew and P. Lankford for their technical assistance. This work is supported by the National Science Foundation, Grant No. DMR 8913854.

- 
- <sup>1</sup>E. L. Wolf, *Principle of Electron Tunneling Spectroscopy* (Oxford Univ. Press, New York, 1989).
- <sup>2</sup>Vladimir Z. Kresin and Stuart A. Wolf, *Phys. Rev. B* **41**, 4278 (1990).
- <sup>3</sup>T. T. M. Palstra, B. Battlog, L. F. Schneemeyer, R. B. Van Dover, and J. F. Waszczak, *Phys. Rev. B* **38**, 5102 (1988).
- <sup>4</sup>H. J. Tao, Farun Lu, and E. L. Wolf (unpublished).
- <sup>5</sup>J. Geerk, G. Linker, O. Meyer, Q. Li, R.-L. Wang, and X. X. Xi, *Physica C* **162-164**, 837 (1989).
- <sup>6</sup>A. Kussmaul, J. S. Moodera, G. M. Roesler, Jr., and P. M. Tedrow, *Phys. Rev. B* **41**, 842 (1990).
- <sup>7</sup>Hiroshi Ikuta, Astutaka Maeda, Kunimitsu Uchinokura, and Shoji Tanaka, *Jpn. J. Appl. Phys.* **27**, L1038 (1988).
- <sup>8</sup>D. Mandrus, L. Forro, D. Koller, and L. M. Mihaly, *Nature (London)* **351**, 460 (1991).
- <sup>9</sup>T. Ekino and J. Akimitsu, *Phys. Rev. B* **40**, 6902 (1989).
- <sup>10</sup>Hongjie Tao, Yingfei Chen, Shipping Zhao, Yifeng Yan, and Qiansheng Yang, *Physica C* **162-164**, 1127 (1989).
- <sup>11</sup>Tetsuya Hasegawa, Masashi Nantoh, and Koichi Kitazawa, *Jpn. J. Appl. Phys.* **30**, L276 (1991).
- <sup>12</sup>M. Boekholt, M. Hoffmann, and G. Gunthrod, *Physica C* **175**, 127 (1991).
- <sup>13</sup>Qun Chen and K.-W. Ng (unpublished).
- <sup>14</sup>Chen Wang, B. Giambattista, C. G. Slough, R. V. Coleman, and M. A. Subramanian, *Phys. Rev. B* **42**, 8890 (1990).
- <sup>15</sup>G. Briceno and Z. Zettl, *Solid State Commun.* **70**, 1055 (1989).
- <sup>16</sup>Nobuaki Miyakawa, Daisuke Shimada, Tadaharu Kido, and Nobuo Tsuda, *J. Phy. Soc. Jpn.* **59**, 2473 (1990).
- <sup>17</sup>S. I. Vedenev and V. A. Stepanov, *Physica C* **162-164**, 1131 (1989).
- <sup>18</sup>M. F. Crommie, G. Briceno, and A. Zettl, *Physica C* **162-164**, 1397 (1989).
- <sup>19</sup>D. M. Mitzi, L. W. Lombardo, A. Kapitulnik, S. S. Ladermann, and R. D. Jacowitz, *Phys. Rev. B* **41**, 6564 (1990).
- <sup>20</sup>J. R. Kirtley and D. J. Scalapino, *Phys. Rev. Lett.* **65**, 798 (1990).
- <sup>21</sup>M. Gurvitch, J. M. Valles, Jr., A. M. Cucolo, R. C. Dynes, J. P. Garno, L. F. Schneemeyer, and J. V. Waszczak, *Phys. Rev. Lett.* **63**, 1008 (1989).
- <sup>22</sup>Siyuan Han, K. W. Ng, E. L. Wolf, H. F. Braun, Lee Tanner, Z. Fisk, J. L. Smith, and M. R. Beasley, *Phys. Rev. B* **32**, 7567 (1985).